

# Discontinuous Galerkin Method for Total Variation Minimization on Inpainting Problem

Xijian Wang

**Abstract**—This paper is concerned with the numerical minimization of energy functionals in  $BV(\Omega)$  (the space of bounded variation functions) involving total variation for gray-scale 1-dimensional inpainting problem. Applications are shown by finite element method and discontinuous Galerkin method for total variation minimization. We include the numerical examples which show the different recovery image by these two methods.

**Keywords**—finite element method, discontinuous Galerkin method, total variation minimization, inpainting

## I. INTRODUCTION

In the first chapter of the book [1] Holger Rauhut has already introduced that the minimization of  $\ell_1$ -norms occupies a fundamental role for the promotion of sparse solutions. This understanding furnishes an important interpretation of total variation minimization [2] as a regularization technique for image inpainting. In this paper we consider as in [3], [4] the minimization in  $BV(\Omega)$  (the space of bounded variation functions [5], [6]) of the functional

$$\mathcal{J}(u) := \int_{\Omega} |Tu(x) - g(x)|^2 dx + 2\lambda |Du|(\Omega), \quad (1)$$

where  $\Omega \subset \mathbb{R}^d$ , for  $d = 1, 2$  be a bounded Lipschitz domain,  $T : L^2(\Omega) \rightarrow L^2(\Omega)$  is a bounded linear operator,  $g \in L^2(\Omega)$  is a datum,  $|Du|(\Omega) := \int_{\Omega} |\nabla u(x)| dx$  is the total variation of  $u$ , and  $\lambda > 0$  is a fixed regularization parameter [7]. Several numerical strategies to efficiently perform total variation minimization have been proposed in the literature, refer to [8], [9], [10], [11]. The crucial difficulty is the correct numerical treatment of interfaces, with the preservation of crossing discontinuities and the correct matching where the solution is continuous instead, see Section 7.1.1 in [12]. In order to deal promptly with the discontinuity, we have studied the applications to gray-scale 1-dimensional inpainting problem by the finite element method and discontinuous Galerkin method (Refer to [13], [14]) for total variation minimization, respectively.

## II. EULER-LAGRANGE EQUATION AND A RELAXATION ALGORITHM

In this section we propose a method for solving the total variation minimization problem (1) in 1-dimensional case. The

Xijian Wang is with the School of Mathematics and Computer Science, Wuyi University, Guangdong, People's Republic of China, 529020 e-mail: wangxj1980426@gmail.com.

details could be found in [15]. For gray-scale 1-dimensional inpainting problem, the functional (1) becomes

$$\mathcal{J}(u) := \int_{\Omega} |1_{\Omega \setminus D}(u(x) - g(x))|^2 dx + 2\lambda \int_{\Omega} |u'(x)| dx, \quad (2)$$

where  $D \subset \Omega$  is the damaged domain with  $\mu(\Omega \setminus D) > 0$ , and  $1_{\Omega \setminus D}$  denotes the characteristic function of  $\Omega \setminus D$ .

Associated to  $\mathcal{J}$  we have the formal Euler-Lagrange equation:

$$-\lambda \left( \frac{u'}{|u'|} \right)' + (u - g)1_{\Omega \setminus D} = 0, \quad (3)$$

with suitable boundary conditions. In our case, we use Neumann conditions.

Later we introduce a new functional given by

$$\varepsilon_h(u, w) = 2 \int_{\Omega} |1_{\Omega \setminus D}(u(x) - g(x))|^2 dx + 2\lambda \int_{\Omega} (w |u'|^2 + \frac{1}{w}), \quad (4)$$

where  $u \in W^{1,2}(\Omega; \mathbb{R})$ , and  $w \in L^2(\Omega; \mathbb{R})$  is such that  $\epsilon_h \leq w \leq \frac{1}{\epsilon_h}$ , where  $\{\epsilon_h\}$  is a positive decreasing sequence such that  $\lim_{h \rightarrow \infty} \epsilon_h = 0$ . While the variable  $u$  again is the function to be reconstructed, we call the variable  $w$  the gradient weight.

For any given  $u^{(0)}$  and  $w^{(0)}$ , we define the following iterative alternating-minimization algorithm:

$$\begin{cases} u^{(n+1)} = \arg \min_{u \in W^{1,2}(\Omega; \mathbb{R})} \varepsilon(u, w^{(n)}), \\ w^{(n+1)} = \arg \min_{\epsilon_h \leq w \leq \frac{1}{\epsilon_h}} \varepsilon(u^{(n+1)}, w). \end{cases} \quad (5)$$

Then we have the 1-dimensional convergent result of Theorem 7.2 in [15].

**Theorem 1:** The sequence  $\{u^{(n)}\}_{n \in \mathbb{N}}$  has subsequences that converge strongly in  $L^2(\Omega; \mathbb{R})$  and weakly in  $W^{1,2}(\Omega; \mathbb{R})$  to a stationary point  $u^{(\infty)}$  of  $\mathcal{J}$ ; i.e.,  $u^{(\infty)}$  solves the Euler-Lagrange equations (3). Moreover, if  $\mathcal{J}$  has a unique minimizer  $u^*$ , then  $u^{(\infty)} = u^*$  and the full sequence  $\{u^{(n)}\}_{n \in \mathbb{N}}$  converges to  $u^*$ .

From **Theorem 1** we conclude that both  $\mathcal{J}$  and  $\varepsilon_h(\cdot, w)$  admit minimizers, their uniqueness is equivalent to the uniqueness of the solutions of the corresponding Euler-Lagrange equation (3). If uniqueness of the solution is satisfied, then the algorithm (5) can be reformulated equivalently as the following two-step iterative procedure:

- Find  $u^{(n+1)}$ , which solves

$$\int_{\Omega} (w^{(n)}(u^{(n+1)})' v' + \frac{1_{\Omega \setminus D}}{\lambda} (u^{(n+1)} - g)v) dx = 0, \quad (6)$$

$\forall v \in W^{1,2}(\Omega; R);$

- Compute directly  $w^{(n+1)}$  by

$$w^{(n+1)} = \epsilon_h \vee \frac{1}{|(u^{(n+1)})'|} \wedge \frac{1}{\epsilon_h}$$

$$:= \begin{cases} \frac{1}{|(u^{(n+1)})'|} & \text{if } \epsilon_h \leq \frac{1}{|(u^{(n+1)})'|} < \frac{1}{\epsilon_h}, \\ \epsilon_h & \text{if } \frac{1}{|(u^{(n+1)})'|} < \epsilon_h < \frac{1}{\epsilon_h}, \\ \frac{1}{\epsilon_h} & \text{otherwise.} \end{cases}$$

In the following sections we illustrate the finite element approximation of the Euler-Lagrange equation (3) similar to [15, section 8]. However, the interesting solutions may be discontinuous. In order to deal promptly with the discontinuity, we have studied the applications to gray-scale 1-dimensional inpainting problem by discontinuous Galerkin method for total variation minimization.

### III. FINITE ELEMENT METHOD FOR TOTAL VARIATION MINIMIZATION

#### A. Finite element method formulation for problem (3).

Denote  $\tilde{\lambda} = \frac{1_{\Omega \setminus D}}{\lambda}$ , then for a given gradient weight  $w^{(n)}$ , the finite element method for solving (5) is to find  $u^{(n+1)}$  such that

$$a(u^{(n+1)}, v) = \langle F, v \rangle \quad \forall v \in W^{1,2}(\Omega; R), \quad (7)$$

where

$$a(u^{(n+1)}, v) = \int_{\Omega} (w^{(n)}(u^{(n+1)})' v' + \tilde{\lambda} u^{(n+1)} v) dx$$

and

$$\langle F, v \rangle = \int_{\Omega} \tilde{\lambda} g v dx.$$

Suppose the problem domain  $\Omega$  is discretized into  $N$  equal size of elements:

$0 = x_0 = x_1 < \dots < x_N = 1$ , denote  $I_m = (x_m, x_{m+1})$  and  $h$  the mesh size. The integral for the  $m^{th}$  element is

$$\int_{x_m}^{x_{m+1}} (w^{(n)}(u^{(n+1)})' v' + \tilde{\lambda} u^{(n+1)} v) dx.$$

The trial function  $u$  is expressed as

$$u^{(n+1)} = \phi_1 u_m^{(n+1)} + \phi_2 u_{m+1}^{(n+1)}$$

with the usual nodal basis functions

$$\phi_1(x) = \frac{x_{m+1} - x}{h}; \quad \phi_2(x) = \frac{x - x_m}{h}.$$

In our example (Section V), the value of  $g$  in each element is a constant (we denote it by  $\tilde{g}$ ) and the value of  $\lambda$  is either 0 or  $\frac{1}{\lambda}$ . Now we could compute the element matrix and the element load vector

$$\mathbf{A}_m^{(n+1)} = w^{(n)} \begin{pmatrix} \frac{1}{h} & -\frac{1}{h} \\ -\frac{1}{h} & \frac{1}{h} \end{pmatrix} + \tilde{\lambda} \begin{pmatrix} \frac{h}{3} & \frac{h}{6} \\ \frac{h}{6} & \frac{h}{3} \end{pmatrix};$$

$$\mathbf{b}_m^{(n+1)} = \tilde{\lambda} \tilde{g} \begin{pmatrix} \frac{h}{2} \\ \frac{h}{2} \end{pmatrix}.$$

Assembling the element matrices and element load vectors, we could obtain the linear system  $\mathbf{A}^{(n+1)} \mathbf{u}^{(n+1)} = \mathbf{b}^{(n+1)}$ .

#### B. Numerical implementation of the alternating-minimization algorithm.

**Input:** Data vector  $\bar{g}$ ,  $\epsilon_h > 0$ , initial gradient weight  $w^{(0)}$  with  $\epsilon_h \leq w^{(0)} \leq \frac{1}{\epsilon_h}$ , number  $n_{max}$  of outer iterations.

**Parameters:** Positive weight  $\tilde{\lambda}$ .

**Output:** Approximation  $u^*$  of the minimizer of (2).

$\mathbf{u}^{(0)} := 0;$

for  $n := 0$  to  $n_{max}$  do

Compute  $\mathbf{u}^{(n+1)}$  such that  $\mathbf{A}^{(n+1)} \mathbf{u}^{(n+1)} = \mathbf{b};$

Compute the gradient

$$(u^{(n+1)}|_{I_m})' = u_m^{(n+1)} \phi_1' + u_{m+1}^{(n+1)} \phi_2' = -\frac{u_m^{(n+1)}}{h} + \frac{u_{m+1}^{(n+1)}}{h};$$

$$w^{(n+1)} = \epsilon_h \vee \frac{1}{|(u^{(n+1)})'|} \wedge \frac{1}{\epsilon_h};$$

endfor

$u^* := u^{(n+1)}.$

### IV. DISCONTINUOUS GALERKIN METHOD FOR TOTAL VARIATION MINIMIZATION

#### A. Discontinuous Galerkin method

In this section, we will use Discontinuous Galerkin method to solve the same problem computing the solution of Euler-Lagrange equation (3). Let us consider the problem

$$-(wu')' + \tilde{\lambda} u = \tilde{\lambda} g \quad (8)$$

Now the DG methods for solving (8) is to find  $u \in \mathcal{D}_1$  such that

$$a(u, v) = \langle F, v \rangle \quad \forall v \in \mathcal{D}_1, \quad (9)$$

where

$$a(u, v) = \sum_{n=0}^{N-1} \int_{x_n}^{x_{n+1}} (wu'v' + \tilde{\lambda} uv) - \sum_{n=0}^N \{w(x_n)u'(x_n)\}[v(x_n)]$$

$$+ \beta \sum_{n=0}^N \{w(x_n)v'(x_n)\}[u(x_n)] + J_0(u, v)$$

is the DG bilinear form, and

$$\langle F, \cdot \rangle = \int_0^1 \tilde{\lambda} g v + \beta (-w(x_0)v'(x_0)u(x_0) + w(x_N)v'(x_N)u(x_N))$$

$$+ \frac{\alpha}{h} (u(x_0)v(x_0) + u(x_N)v(x_N))$$

is the linear form. In our example (Section V), we take the parameter  $\beta = 1$  so that the DG bilinear form is symmetric.

#### B. Linear system

In this subsection, we derive the linear system obtained from the DG method. We choose for local basis functions of  $P_1(I_n)$  the nodal basis functions, i.e,  $P_1(I_n) = \text{span}\{\phi_1^n, \phi_2^n\}$  with

$$\phi_1^n(x) = \frac{x_{i+1} - x}{x_{i+1} - x_i}; \quad \phi_2^n(x) = \frac{x - x_i}{x_{i+1} - x_i}.$$

The global basis functions  $\{\Phi_i^n\}$  for the space  $\mathcal{D}_1$  are obtained from the local basis functions by extending them by zero:

$$\Phi_i^n(x) = \begin{cases} \phi_i^n(x) & \text{if } x \in I_n, \\ 0 & \text{otherwise.} \end{cases}$$

We can then expand the DG solution as

$$u^{DG}(x) = \sum_{m=0}^{N-1} \sum_{j=1}^2 \alpha_j^m \Phi_j^m(x). \quad (10)$$

Inserting this form of  $u^{DG}$  into the scheme (9), we get

$$\sum_{m=0}^{N-1} \sum_{j=1}^2 \alpha_j^m a(\Phi_j^m, \Phi_i^n) = \langle F, \Phi_i^n \rangle,$$

for  $0 \leq n \leq N-1$  and  $1 \leq i \leq 2$ . We would then obtain a linear system  $\mathbf{A}\alpha = \mathbf{b}$ , where  $\alpha$  is the vector with components  $\alpha_j^m$ ,  $\mathbf{A}$  is the matrix with entries  $a(\Phi_j^m, \Phi_i^n)$ , and  $\mathbf{b}$  is the vector with the components  $\langle F, \Phi_i^n \rangle$ .

1) **Computing the matrix  $\mathbf{A}$ :** In this section, we will first show how to compute the local matrices. We will regroup the terms  $a(\Phi_j^m, \Phi_i^n)$  into three groups: the terms involving integrals over  $I_n$ , the terms involving the interior nodes  $x_n$ , and the terms involving the boundary nodes  $x_0$  and  $x_N$ .

Firstly, we consider the term corresponding to the integrals over  $I_n$ . On each element  $I_n$ , the DG solution  $u^{DG}$  can be expressed as

$$u^{DG}(x) = \alpha_1^n \phi_1^n(x) + \alpha_2^n \phi_2^n(x) \quad \forall x \in I_n. \quad (11)$$

Thus, using (11) and choosing  $v = \phi_i^n$  for  $i = 1, 2$ , we get

$$\begin{aligned} & \int_{x_n}^{x_{n+1}} (w(u^{DG})'(\phi_i^n))' + \tilde{\lambda} u^{DG} \phi_i^n dx \\ &= \sum_{j=1}^2 \alpha_j^n \int_{x_n}^{x_{n+1}} (w(\phi_j^n)'(\phi_i^n))' + \tilde{\lambda} \phi_j^n \phi_i^n dx \quad \forall i = 1, 2. \end{aligned}$$

This linear system can be written as  $\mathbf{A}_n \alpha^n$ , where

$$(\mathbf{A}_n)_{ij} = \int_{x_n}^{x_{n+1}} (w(\phi_j^n)'(\phi_i^n))' + \tilde{\lambda} \phi_j^n \phi_i^n dx, \quad \alpha^n = \begin{pmatrix} \alpha_1^n \\ \alpha_2^n \end{pmatrix}.$$

We could compute the  $\mathbf{A}_n$ :

$$\mathbf{A}_n = \frac{w_n}{h} \begin{pmatrix} 1 & -1 \\ -1 & 1 \end{pmatrix} + \tilde{\lambda} h \begin{pmatrix} 1/3 & 1/6 \\ 1/6 & 1/3 \end{pmatrix}.$$

Second, we consider the terms involving the interior nodes  $x_n$ . Let us express

$$\begin{aligned} & -\{w(x_n)(u^{DG})'(x_n)\}[v(x_n)] + \beta\{w(x_n)v'(x_n)\}[u^{DG}(x_n)] \\ & + \frac{\alpha}{h}[u^{DG}(x_n)][v(x_n)] = b_n + c_n + d_n + e_n, \end{aligned}$$

where the terms are defined as below:

$$\begin{aligned} b_n &= \frac{1}{2}w(x_n^+)(u^{DG})'(x_n^+)v(x_n^+) - \frac{\beta}{2}w(x_n^+)u^{DG}(x_n^+)v'(x_n^+) \\ &+ \frac{\alpha}{h}u^{DG}(x_n^+)v'(x_n^+), \end{aligned}$$

$$\begin{aligned} c_n &= -\frac{1}{2}w(x_n^-)(u^{DG})'(x_n^-)v(x_n^-) + \frac{\beta}{2}w(x_n^-)u^{DG}(x_n^-)v'(x_n^-) \\ &+ \frac{\alpha}{h}u^{DG}(x_n^-)v'(x_n^-), \end{aligned}$$

$$\begin{aligned} d_n &= -\frac{1}{2}w(x_n^+)(u^{DG})'(x_n^+)v(x_n^-) - \frac{\beta}{2}w(x_n^-)u^{DG}(x_n^+)v'(x_n^-) \\ &- \frac{\alpha}{h}u^{DG}(x_n^+)v'(x_n^-), \end{aligned}$$

$$\begin{aligned} e_n &= \frac{1}{2}w(x_n^-)(u^{DG})'(x_n^-)v(x_n^+) + \frac{\beta}{2}w(x_n^+)u^{DG}(x_n^-)v'(x_n^+) \\ &- \frac{\alpha}{h}u^{DG}(x_n^-)v'(x_n^+). \end{aligned}$$

Now with the expression (11) and the choice  $v = \phi_i^n$ , the four terms defined above yields the local matrices  $\mathbf{B}_n, \mathbf{C}_n, \mathbf{D}_n$  and  $\mathbf{E}_n$  which are:

$$\begin{aligned} \mathbf{B}_n &= \frac{1}{2h} \begin{pmatrix} -w(x_n^+) + \beta w(x_n^+) + 2\alpha & w(x_n^+) \\ -\beta w(x_n^+) & 0 \end{pmatrix}, \\ \mathbf{C}_n &= \frac{1}{2h} \begin{pmatrix} 0 & -\beta w(x_n^-) \\ w(x_n^-) & -w(x_n^-) + \beta w(x_n^-) + 2\alpha \end{pmatrix}, \\ \mathbf{D}_n &= \frac{1}{2h} \begin{pmatrix} \beta w(x_n^-) & 0 \\ w(x_n^+) - \beta w(x_n^-) - 2\alpha & -w(x_n^+) \end{pmatrix}, \\ \mathbf{E}_n &= \frac{1}{2h} \begin{pmatrix} -w(x_n^-) & w(x_n^-) - \beta w(x_n^+) - 2\alpha \\ 0 & \beta w(x_n^+) \end{pmatrix}. \end{aligned}$$

Finally, we compute the local matrices from the boundary nodes  $x_0$  and  $x_N$ :

$$\begin{aligned} f_0 &= w(x_0)(u^{DG})'(x_0)v(x_0) - \beta w(x_0)u^{DG}(x_0)v'(x_0) \\ &+ \frac{\alpha}{h}u^{DG}(x_0)v'(x_0), \end{aligned}$$

$$\begin{aligned} f_N &= -w(x_N)(u^{DG})'(x_N)v(x_N) + \beta w(x_N)u^{DG}(x_N)v'(x_N) \\ &+ \frac{\alpha}{h}u^{DG}(x_N)v'(x_N), \end{aligned}$$

which yields the local matrices  $\mathbf{F}_0$  and  $\mathbf{F}_N$ :

$$\begin{aligned} \mathbf{F}_0 &= \frac{1}{h} \begin{pmatrix} -w(x_0) + \beta w(x_0) + \alpha & w(x_0) \\ -\beta w(x_0) & 0 \end{pmatrix}, \\ \mathbf{F}_N &= \frac{1}{h} \begin{pmatrix} 0 & -\beta w(x_N) \\ w(x_N) & -w(x_N) + \beta w(x_N) + \alpha \end{pmatrix}. \end{aligned}$$

Assuming that the unknowns are listed in the following order:

$$(\alpha_1^0, \alpha_2^0, \alpha_1^1, \alpha_2^1, \alpha_1^2, \alpha_2^2, \dots, \alpha_1^{N-1}, \alpha_2^{N-1}),$$

we obtain the global matrix  $\mathbf{A}$  which is block tridiagonal

$$\mathbf{A} = \begin{pmatrix} \mathbf{M}_0 & \mathbf{D}_1 & & & \\ \mathbf{E}_1 & \mathbf{M} & \mathbf{D}_2 & & \\ & \dots & \dots & \dots & \\ & & \dots & \dots & \dots \\ & & & \mathbf{E}_{N-2} & \mathbf{M} & \mathbf{D}_{N-1} \\ & & & & \mathbf{E}_{N-1} & \mathbf{M}_N \end{pmatrix},$$

where

$$\begin{aligned} \mathbf{M} &= \mathbf{A}_n + \mathbf{B}_n + \mathbf{C}_{n+1}, \mathbf{M}_0 = \mathbf{A}_0 + \mathbf{F}_0 + \mathbf{C}_1, \\ \mathbf{M}_N &= \mathbf{A}_{N-1} + \mathbf{F}_N + \mathbf{C}_{N-1}. \end{aligned}$$

2) **Computing the right hand side  $\mathbf{b}$ :** Each component of  $\mathbf{b}$  can be obtained by computing

$$\begin{aligned} \langle F, \Phi_i^n \rangle &= \int_0^1 \tilde{\lambda} g \Phi_i^n dx + \beta(-w(x_0)(\Phi_i^n)'(x_0)u(x_0) \\ &+ w(x_N)(\Phi_i^n)'(x_N)u(x_N)) \\ &+ \frac{\alpha}{h}(u(x_0)\Phi_i^n(x_0) + u(x_N)\Phi_i^n(x_N)). \end{aligned}$$

Because of the local support of  $\Phi_n^i$ , the first term is reduced to

$$\int_0^1 \tilde{\lambda} g \Phi_n^i dx = \int_{x_n}^{x_{n+1}} \tilde{\lambda} g \phi_n^i dx.$$

We arrange the components of  $\mathbf{b}$  in an order consistent with the order of the unknowns  $\alpha_i^n$ :

$$(b_1^0, b_2^0, b_1^1, b_2^1, b_1^2, b_2^2, \dots, b_1^{N-1}, b_2^{N-1}),$$

where the first two components and last two components are

$$\begin{aligned} b_1^0 &= \frac{\tilde{\lambda} g_0 h}{2} + \frac{\beta w(x_0) u(x_0)}{h} + \frac{\alpha u(x_0)}{h}, \\ b_2^0 &= \frac{\tilde{\lambda} g_0 h}{2} - \frac{\beta w(x_0) u(x_0)}{h}, \\ b_1^{N-1} &= \frac{\tilde{\lambda} g_{N-1} h}{2} - \frac{\beta w(x_N) u(x_N)}{h}, \\ b_2^{N-1} &= \frac{\tilde{\lambda} g_{N-1} h}{2} + \frac{\beta w(x_N) u(x_N)}{h} + \frac{\alpha u(x_N)}{h}, \end{aligned}$$

and the other  $2(N-2)$  components are

$$b_i^n = \frac{\tilde{\lambda} g_n h}{2}, \quad \forall 1 \leq n \leq N-2, \forall 1 \leq i \leq 2.$$

## V. NUMERICAL EXAMPLES AND FUTURE STUDY

We would first use finite element method for total variation minimization the do some experiments with different values of parameter  $\tilde{\lambda}$  in the alternating minimization algorithm. Let us consider the same signal with the same inpainting interval  $(\frac{1}{3}, \frac{2}{3})$ , see Fig.1. We conclude that quality of the recovery image is becoming better as the value of  $\tilde{\lambda}$  increases.

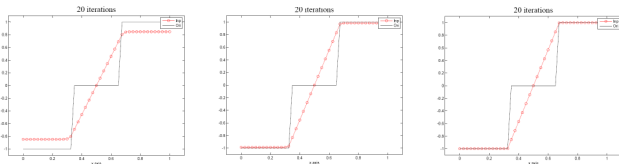


Fig.1 The three pictures from left to right represent the result of three different values of  $\tilde{\lambda}$  ( $\tilde{\lambda} = 10, 100, 1000$ ), respectively.

Second, we fix the outer iteration to 20 and compare the convergence speed for three different values of  $\tilde{\lambda}$  ( $\tilde{\lambda} = 10, 100, 1000$ ), see the left picture of Fig.2. And we conclude that the convergence speed increases as the value of  $\tilde{\lambda}$  increases.

Finally, we modify  $w^{(n+1)}$  from  $\epsilon_h \vee \frac{1}{|(u^{(n+1)})'|} \wedge \frac{1}{\epsilon_h}$  to  $(\epsilon_h \vee \frac{1}{|(u^{(n+1)})'|})^{2-\tau}$ , and check the convergence speed for different value of  $\tau$  ( $\tau=1, 0.9, 0.8, 0.7, 0.6, 0.5$ ). The result is shown in the right picture of Fig.2. And we conclude that the convergence speed increases as the value of  $\tau$  decreases.

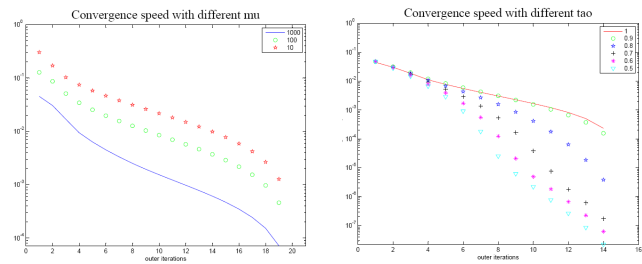


Fig.2 The left picture illustrates the convergence speed for three different values of  $\tilde{\lambda}$  ( $\tilde{\lambda} = 10, 100, 1000$ ); the right picture shows the convergence speed for different value of  $\tau$  ( $\tau=1, 0.9, 0.8, 0.7, 0.6, 0.5$ ).

Next we consider a signal with a jump (see Fig.3).

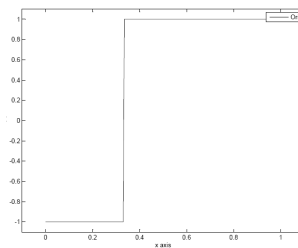


Fig.3 The signal of a step function.

Let us recover the signal(Fig.3) by finite element method and discontinuous Galerkin method for total variation, respectively. The results are shown in Fig.4. We observe that the finite element method for total variation minimization couldn't preserve the jump very well from our example. However, the discontinuous Galerkin method for total variation minimization preserves the jump rather well.

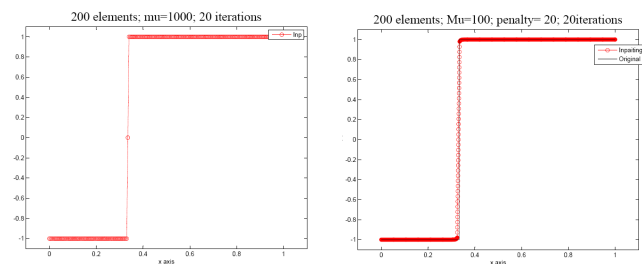


Fig.4 The left picture shows the recovery image by the finite element method for total variation minimization; and the right picture illustrates discontinuous Galerkin method for total variation minimization.

Our future study aims at the construction, analysis and implementation of new adaptive discontinuous Galerkin (DG) solvers for total variation minimization problems in two space dimensions. These methods are based on re-weighted least squares and are implemented by nester outer and inner iterations. The adaptivity concerns not only the space discretization but also the parameters involved in the inner and outer iterations as well as in the DG discretization.

## ACKNOWLEDGMENT

The author wishes to thank the financial support from Erasmus Mundus Scholarship of European Union and thank Dr. Massimo Fornasier and Prof. Dr. Ulrich Langer for their valuable suggestions during the Project discussion on Numerical Analysis in Johannes Kepler Linz University, Austria.

## REFERENCES

- [1] M. Fornasier, *Theoretical Foundations and Numerical Methods for Sparse Recovery*, De Gruyter, 2010.
- [2] L. Rudin, S. Osher, E. Fatemi, *Nonlinear total variation based noise removal algorithms*, Physica D 60 (1992) 259–268.
- [3] A. Chambolle, P.-L. Lions, *Image recovery via total variation minimization and related problems*, Numer Math. 76 (1997) 167–188.
- [4] L. Vese, *A study in the BV space of a denoising-deblurring variational problem*, Appl. Math. Optim. 44 (2001) 131–161.
- [5] G. Aubert, P. Kornprobst, *Mathematical Problems in Image Processing. Partial Differential Equations and the Calculus of Variation*, Springer, 2006.
- [6] T. Chan, J. Shen, *Image Processing and Analysis: Variational, PDE, Wavelet, and Stochastic Methods*, SIAM, 2005.
- [7] H. W. Engl, M. Hanke, A. Neubauer, *Regularization of inverse problems*, Kluwer Academic Publishers, Dordrecht, The Netherlands 76 (1996).
- [8] A. Chambolle, J. Darbon, *On total variation minimization and surface evolution using parametric maximum flows*, International Journal of Computer Vision 84 (2009) no. 3, 288–307.
- [9] T. Goldstein, S. Osher, *The split bregman method for  $L^1$  regularized problems*, SIAM Journal on Imaging Sciences 2 (2009) no. 2, 323–343.
- [10] S. Osher, M. Burger, D. Goldfarb, J. Xu, W. Yin, *An iterative regularization method for total variation-based image restoration*, Multiscale Model. Simul. 4 (2005) no. 2, 460–489.
- [11] P. Weiss, L. Blanc-Féraud, G. Aubert, *Efficient schemes for total variation minimization under constraints in image processing*, SIAM J. Sci. Comput. 31 (2009) no. 3, 2047–2080.
- [12] M. Fornasier, C. Schönlieb, *Subspace correction methods for total variation and  $\ell_1$ -minimization*, SIAM J. Numer. Anal. 47 (2009) no.5, 3397–3428.
- [13] B. Cockburn, G. E. Karniadakis, C.-W. Shu, *Discontinuous Galerkin Methods: Theory, Computation and Applications*, Springer, 2000.
- [14] B. Rivière, *Discontinuous Galerkin Methods For Solving Elliptic and Parabolic Equations: Theory and Implementation*, SIAM, 2008.
- [15] M. Fornasier, R. March, *Restoration of color images by vector valued BV functions and variational calculus*, SIAM J. Appl. Math. 68 (2007) 437–460.